Mathematical Biosciences and Engineering

http://www.aimspress.com/journal/mbe

MBE, 20(2): 1558–1579.
DOI: 10.3934/mbe.2023071
Received: 13 September 2022
Revised: 19 October 2022
Accepted: 27 October 2022
Published: 03 November 2022

Research article

A fishery predator-prey model with anti-predator behavior and complex dynamics induced by weighted fishing strategies

Yuan Tian[1,*], **Yan Gao**[1] **and Kaibiao Sun**[2]

[1] School of Science, Dalian Maritime University, Dalian 116026, China
[2] School of Control Science and Engineering, Dalian University of Technology, Dalian 116024, China

* **Correspondence:** Email: tianyuan@dlmu.edu.cn, tianyuan1981@163.com.

Abstract: In this work, a fishery predator-prey model with anti-predator behavior is presented according to the anti-predator phenomenon in nature. On the basis of this model, a capture model guided by a discontinuous weighted fishing strategy is established. For the continuous model, it analyzes how anti-predator behavior affects system dynamics. On this basis, it discusses the complex dynamics (order-m periodic solution ($m = 1, 2$)) induced by a weighted fishing strategy. Besides, in order to find the capture strategy that maximizes the economic profit in the fishing process, this paper constructs an optimization problem based on the periodic solution of the system. Finally, all of the results of this study have been verified numerically in MATLAB simulation.

Keywords: periodic solution; weighted fishing strategy; anti-predator behavior; optimization

1. Introduction

In nature, there are many predator-prey relationships among various organisms, and this is also the reason for the balance of nature. This relationship has gone through a long process of natural evolution. Predators and prey have formed various adaptations of predation and anti-predation in structure, physiology, habits and lifestyle, forming a certain balanced relationship. In 2012, Choh et al. [1] found a phenomenon in an experiment that there is a role reversal (anti-predator behavior) between predators and prey. When the prey species were threatened, in order to survive and reproduce, they will fight back, and even kill the predators' juveniles. In 2013, Hoover et al. [2] revealed that fathead minnows exhibit typical anti-predator behavior; as a response to the predator scent signatures and chemical alarm cues, they will go into shelters and decrease activity. In 2015, O'Connor et al. [3] revealed that stimulated by the predators, cichlid fish species spend less time exploring and more time searching for cover and congregating with other similar species to avoid being attacked by predators.

In addition, researchers have revealed that in the presence of predation hazards, many species such as the three-spined stickleback [4], monkey goby [5], red tilefish [6] and other species will exhibit anti-predator behavior.

To characterize the anti-predator behavior of prey species and analyze its impact on the dynamics of the system, many scholars have introduced the anti-predator effect into the predator-prey model [7, 8, 9, 10, 11, 12]; among others, Tang and Xiao [7] revealed that the predator will go extinct as a consequence of the anti-predator behavior, which means that anti-predator behavior can aid prey species in resisting predator aggressiveness. Sun et at. [8] introduced a kind of anti-predator behavior, which occurs only when the prey group size is larger than a threshold. Mortoja et al. [9] introduced anti-predator behavior into a stage-structure model, and, through numerical simulations, they found that the anti-predator factor may change the system's stability. Prasad [10] analyzed an additional food provided predator-prey system with anti-predator behaviour in prey. Sirisubtawee et al. [11] introduced anti-predator behavior into an impulsive Holling type IV predator-prey model, and discussed the complex dynamics such as the periodic solution of the impulsive model. Tian and Gao [12] presented a predator-prey model with an anti-predation effect and prey-dependent threshold control and analyzed the dynamics of the proposed model.

On the other hand, fishing activities are carried out for both commercial and livelihood needs. However, it is worth pointing out that overfishing will always lead to depletion of fishery resources. Therefore, rational management of fishery resources is necessary from the perspective of renewable resources protection, and appropriate fishing levels can not only protect fishery resources, but also maximize profits. Fishing activities can be carried out in different manners, which include continuous form [13, 14, 15], semi-continuous form [16], periodic form [17, 18] and state-dependent form [19, 20, 21]. Fishing activity is a typical human activity and it is usually determined by the density of the fish population. State-dependent harvesting strategy takes the current state of the species into consideration and avoid the adverse impacts on the sustainability of the species. There are many cases of human intervention in real world problems, which often occur at state-dependent times or involve state-dependent thresholds. For such situations, state-dependent strategies are usually used to model this phenomena or problems, and the corresponding system can be described by impulsive semi-dynamical systems (ISDSs) [22, 23, 24, 25]. In the past two decades, many scholars have applied the theory and method of impulsive semi-dynamic system into different subjects and scientific problems, such as pest control [26, 27, 28, 29, 30], disease control [31, 32], process of sugar manufacturing [33], prey-predator system [34, 35, 36, 37, 38], competitive system [39] and other subjects [40, 41]. Predator-prey systems based on state feedback control had received much attentions, the corresponding models can be divided into predator-dependent [19, 20], prey-dependent [42, 43, 44, 45], ratio-dependent [46, 47] and prey-predator hybrid-dependent [21, 48, 49]. In natural systems, predators and prey are mixed, so it is impossible to determine the exact number of the two species, but their proportions are usually kept constant. Based on this consideration, a weight capture strategy was introduced into a fishery model [21], where fishing activity is permitted when the weighted sum of both species populations reaches a threshold. In the current work, we present a predator-prey model with anti-predator behavior and analyze how anti-predator behavior affects system dynamics. Then, following application of the weight capture strategy to the system, we analyze the complex dynamics induced by a discontinuous weighted fishing strategy. In addition, in order to obtain the optimal fishing strategy that maximizes economic profits, we discuss the problem of fishing process optimization.

The article structure is as follows. In Section 2, we propose a predator-prey model for fisheries with anti-predator behavior and construct a capture model based on weighted fishing strategies, followed by presenting some basic knowledge. In the next section, we first investigate the effects of anti-predator behavior on system dynamics, and then discuss the complex dynamics of the system induced by a weighted fishing strategy. In addition, in order to maximize the economic profit, we carried out the study of the optimization of the fishing process. In Section 4, we discuss the numerical simulations performed to verify the theoretical results obtained in the previous section. In the last section, we present a summary and discussion.

2. Mathematical model and basic knowledge

Let x denote the prey density and y denote the predator density. Then the classical predator-prey model can be expressed as follows:

$$\begin{cases} \dfrac{\mathrm{d}x}{\mathrm{d}t} = B(x) - yD(x), \\ \dfrac{\mathrm{d}y}{\mathrm{d}t} = \mu yD(x) - sy, \end{cases} \tag{2.1}$$

where, $B(x)$ describes the prey growth rate, $D(x)$ represents the functional response, s represents the predator mortality rate and μ denotes the conversion rate from prey to predator. In this study, the logistic type growth rate and Holling-II type functional response are considered, i.e., $B(x) = rx(1 - x/K)$ and $D(x) = bx/(1 + h_1 x)$.

When the prey species shows anti-predator behavior, let p characterize the anti-predator rate of the prey; the term $-pxy$ is added to the change rate of predators. Then, Model (2.1) takes the form

$$\begin{cases} \dfrac{\mathrm{d}x}{\mathrm{d}t} = rx(1 - \dfrac{x}{K}) - \dfrac{bxy}{1 + h_1 x} := xP(x, y), \\ \dfrac{\mathrm{d}y}{\mathrm{d}t} = \dfrac{\mu bxy}{1 + hx} - sy - pxy := yQ(x), \end{cases} \tag{2.2}$$

where r describes the intrinsic growth rate, K represents the environmental capacity, b denotes the predation rate, h_1 is the saturation constant, $h = h_1 + bh_2$ and h_2 describes the conversion saturation constant. Considering the biological significance of the model, the study is regionally limited in $\Omega_0 = \{(x, y)|0 \leq x \leq K,\ y \geq 0\}$.

For both commercial and livelihood needs, fishing activities are carried out when the fish populations satisfy certain conditions. Let w denote the proportion of prey species, $(1 - w)$ be the proportion of a predator population, H denote the threshold of the weighted sum of both species populations, E represent the capture strength and q_i $(i = 1, 2)$ denotes the capture rate. Besides, in order to prevent the extinction of predators caused by anti-predator behavior, a quantity of predator pups, denoted by τ, is released into the system. Based on the above capture strategies, the predator-prey model guided by the weighted fishing strategy is as follows:

$$\begin{cases} \left.\begin{aligned} \dfrac{\mathrm{d}x}{\mathrm{d}t} &= rx(1 - \dfrac{x}{K}) - \dfrac{bxy}{1 + h_1 x} \\ \dfrac{\mathrm{d}y}{\mathrm{d}t} &= \dfrac{\mu bxy}{1 + hx} - sy - pxy \end{aligned}\right\} wx + (1 - w)y \neq H, \\ \left.\begin{aligned} \Delta x &= -q_1 Ex \\ \Delta y &= -q_2 Ey + \tau \end{aligned}\right\} wx + (1 - w)y = H \end{cases} \tag{2.3}$$

where τ satisfies that $\tau < \min\{\tau_1, \tau_2\}$, and

$$\tau_1 \triangleq \frac{q_2 HE}{1-w},\ \tau_2 \triangleq \frac{q_1 HE}{1-w} \cdot \frac{1-q_2 E}{1-q_1 E}.$$

The research objective of this paper is to analyze how anti-predator behavior affects the dynamics of System (2.2), and also to discuss the complex dynamics of the Model (2.3) induced by a weighted fishing strategy. Besides, to obtain an optimal capture strategy that maximizes the economic profit, we discuss the problem of fishing process optimization.

We present some basic concepts and results of an ISDS for convenience, and the readers are referred to the literature [21, 23, 25, 29, 30, 45].

Let us consider a planar impulsive model with following threshold

$$\begin{cases} \left.\begin{aligned} \frac{\mathrm{d}x}{\mathrm{d}t} &= f_1(x,y) \\ \frac{\mathrm{d}y}{\mathrm{d}t} &= f_2(x,y) \end{aligned}\right\} & \chi(x,y) \neq 0, \\ \left.\begin{aligned} \Delta x &= I_1(x,y) \\ \Delta y &= I_2(x,y) \end{aligned}\right\} & \chi(x,y) = 0, \end{cases} \tag{2.4}$$

where f_i, I_i and χ are differentiable with respect to x and y. Let Ω represent the domain of solutions and $\pi = (\pi_1, \pi_2) : \Omega \times R \to \Omega$ characterize the solution map of the corresponding continuous system; define $\mathcal{M} \triangleq \{(x,y) \in \Omega | \chi(x,y) = 0\}$ and $I = (I_1, I_2)$: $\mathcal{M} \to \mathcal{N} = I(\mathcal{M})$. Then we call the system constituted by (2.4) as an ISDS, which is denoted by $(\Omega, \pi; I, \mathcal{M})$. For any point $S_0 \in \mathcal{N}$, the solution of $(\Omega, \pi; I, \mathcal{M})$ from S_0 is denoted by $\mathbf{z}(t) = (x(t), y(t))'$, i.e. $\mathbf{z}(0) = \mathbf{z}_0 \triangleq S_0$. The orbit is denoted by $\gamma_{S_0}(\mathbf{z}) \triangleq \{\mathbf{z}(t) | t \geq 0, \mathbf{z}(0) = S_0\}$. If $\gamma_{S_0}(\mathbf{z}) \cap \mathcal{M} \neq \emptyset$, the trajectory $\mathbf{z}(t)$ will reach the pulse set $\mathcal{M}$ many times due to the pulse action; the set of the time is denoted by $\Sigma \triangleq \{t_k | k = 1, 2, \cdots\}$, i.e. $\mathbf{z}_k^- = \mathbf{z}(t_k) \in \mathcal{M}$ and $\mathbf{z}_k = I(\mathbf{z}_k^-) \in \mathcal{N}$.

Definition 2.1 (Periodic solution [21, 23, 29, 30, 45])**.** *The solution $\tilde{\mathbf{z}}(t)$ with $\tilde{\mathbf{z}}_0 \in \mathcal{N}$ is said to be periodic if there exists $n \geqslant 1$ satisfying $\tilde{\mathbf{z}}_n = \tilde{\mathbf{z}}_0$. Denote $m \triangleq \min\{k | 1 \leq k \leq n, \tilde{\mathbf{z}}_k = \tilde{\mathbf{z}}_0\}$; then, $\tilde{\mathbf{z}}(t)$ is called an order-m periodic solution with period $T = t_m$.*

Definition 2.2 (Oorbitally asymptotically stable [21, 23, 29, 30, 45])**.** *For the periodic solution $\tilde{\mathbf{z}}(t)$, if for an arbitrary $\epsilon > 0$, there is a neighborhood U_δ of $\tilde{\mathbf{z}}$, for any $\mathbf{z} \in U_\delta$, there exists a re-parameterized function $\hat{t}(t)$ and $|\mathbf{z}(t) - \tilde{\mathbf{z}}(\hat{t}(t))| < \epsilon$ for all $t \geq t_0$; then, $\gamma(\tilde{\mathbf{z}})$ is called orbitally asymptotically stable.*

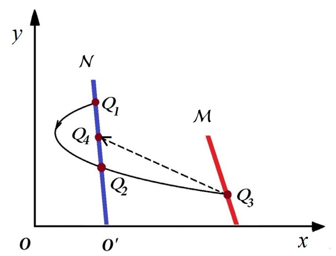

Figure 1. Schematic diagram of successor function.

Definition 2.3 (Successor function [23, 29, 30]). *Let us assume that $\mathcal{M}$ and $\mathcal{N}$ in $(\mathbb{R}^2_+, \pi, \mathbb{R}_+; \mathcal{M}, I)$ are two disjoint lines. Denote $\mathcal{N} \cap x$-axis $= \{O'\}$. For a given $Q_1 \in \mathcal{N}$, denote $\gamma_{Q_1}(\mathbf{z}) \cap \mathcal{M} = \{Q_3\}$, $\gamma_{Q_1}(\mathbf{z}) \cap \mathcal{N} = \{Q_2\}$ and $Q_4 = I(Q_3)$, as illustrated in Figure 1. Then the type-I successor function $f^{\mathrm{I}}_{\mathrm{SOR}}$ is defined by $f^{\mathrm{I}}_{\mathrm{SOR}}(Q_2) = d(Q_4, O') - d(Q_2, O')$, and the type-II successor function $f^{\mathrm{II}}_{\mathrm{SOR}}$ is defined by $f^{\mathrm{II}}_{\mathrm{SOR}}(Q_1) = d(Q_4, O') - d(Q_1, O')$.*

Lemma 2.1 (Stability criterion [21, 23, 29, 30, 45]). *The order-m periodic solution $\mathbf{z}(t) = (\xi(t), \eta(t))'$ with the period T is said to be orbitally asymptotically stable if $|\mu_m| < 1$ holds, where*

$$\mu_m = \prod_{j=1}^{n} \Delta_j \exp\left(\int_0^T \left[\frac{\partial f_1}{\partial x} + \frac{\partial f_2}{\partial y}\right]_{(\xi(t),\eta(t))} dt\right),$$

with

$$\Delta_j = \frac{f_1^+\left(\frac{\partial I_2}{\partial y}\frac{\partial \chi}{\partial x} - \frac{\partial I_2}{\partial x}\frac{\partial \chi}{\partial y} + \frac{\partial \chi}{\partial x}\right) + f_2^+\left(\frac{\partial I_1}{\partial x}\frac{\partial \chi}{\partial y} - \frac{\partial I_1}{\partial y}\frac{\partial \chi}{\partial x} + \frac{\partial \chi}{\partial y}\right)}{f_1\frac{\partial \chi}{\partial x} + f_2\frac{\partial \chi}{\partial y}},$$

$f_1^+ = f_1(\xi(\tau_j^+), \eta(\tau_j^+))$, $f_2^+ = f_2(\xi(\tau_j^+), \eta(\tau_j^+))$ and f_1, f_2, $\frac{\partial I_1}{\partial x}$, $\frac{\partial I_1}{\partial y}$, $\frac{\partial I_2}{\partial x}$, $\frac{\partial I_2}{\partial y}$, $\frac{\partial \chi}{\partial x}$ and $\frac{\partial \chi}{\partial y}$ are calculated at $(\xi(\tau_j), \eta(\tau_j))$.

3. Dynamical analysis of Systems (2.2) and (2.3)

This section focuses on analyzing the dynamics of the free system (2.2) and the capture system (2.3), respectively. Since, in the case of $\mu b \leqslant sh$, there is $\mathrm{d}y/\mathrm{d}t < 0$, i.e., the predator species will eventually become extinct. Therefore, from the perspective of ecological diversity, it is assumed that $\mu b > sh$.

3.1. Dynamics of System (2.2)

For System (2.2), we mainly discuss the existence and stability of equilibria. For convenience, denote

$$F(x) \triangleq \frac{r(1 + h_1 x)(K - x)}{bK},\ p_1 \triangleq ub + sh - 2\sqrt{\mu bsh},\ m \triangleq p + sh - \mu b,$$

$$x_1^p \triangleq \begin{cases} s/(\mu b - sh), & p = 0 \\ \frac{-m-\sqrt{m^2-4phs}}{2ph}, & 0 < p < p_1 \\ \frac{\mu b - p_1 - sh}{2p_1 h}, & p = p_1 \end{cases},\quad x_2^p \triangleq \begin{cases} K, & p = 0 \\ \frac{-m+\sqrt{m^2-4phs}}{2ph}, & 0 < p < p_1 \\ K, & p = p_1 \end{cases}$$

and $y_i^p = F(x_i^p)$, $i = 1, 2$.

Define

$$g(p) = \left(2\frac{h}{h_1} - 1\right)p - sh + \mu b - 3\sqrt{(p + sh - \mu b)^2 - 4ph}.$$

Let $\overline{p} \in (0, p_1)$ satisfy $g(\overline{p}) = 0$. Since the dynamic behavior of System (2.2) are related to the parameters p and K, we divide the analysis into the following three cases:

$(A1)$: $0 \le p \le p_1, x_1^p < K \le x_2^p$;

$(A2)$: $0 < p < p_1, K > x_2^p$;

$(A3)$: $p > p_1$.

Further, $(A1)$ is divided into five subcases:

$(A1\text{-}1)$: $0 \le p \le \overline{p}$, $x_1^p < K \le 2x_1^p + 1/h_1$;

$(A1\text{-}2)$: $0 \le p \le \overline{p}$, $2x_1^p + 1/h_1 < K \le x_2^p$;

$(A1\text{-}3)$: $\overline{p} < p < p_1$, $x_1^p < K \le x_2^p$;

$(A1\text{-}4)$: $p = p_1$, $x_1^p < K \le x_2^p$

and $(A2)$ is divided into three subcases:

$(A2\text{-}1)$: $\overline{p} < p < p_1$, $x_2^p < K < 2x_1^p + 1/h_1$;

$(A2\text{-}2)$: $0 \le p < p_1$, $K > \underline{K} \triangleq \max\{2x_1^p + 1/h_1, x_2^p\}$.

3.1.1. Existence of equilibria

In System (2.2), $E_O(0,0)$ and $E_K(K,0)$ always exist.

Theorem 3.1. *In System* (2.2)*, if Case* $(A1)$ *holds, there exists a unique positive equilibrium* E_1*; if Case* $(A2)$ *holds, there exists two positive equilibria* E_1 *and* E_2*; for Case* $(A3)$*, the positive equilibrium does not exist.*

Proof of Theorem 3.1. Define $Q_0(x) = (1 + hx)Q(x)$. Then, System (2.2) has a positive equilibrium if and only if the equation $Q_0(x) = 0$ has a positive root less than K. Since $Q_0(x) = 0$ does not have a positive root when $p > p_1$, the positive equilibrium does not exist for Case $(A3)$. While, for $0 \le p \le p_1$, we have the following cases:

Case I: $p = 0$. Then $Q_0(x) = 0$ has a unique positive root $x = x_1^0$. Let $y_1^0 = F(x_1^0)$. Then $E_1(x_1^0, y_1^0)$ is a positive equilibrium if $K > x_1^0$;

Case II: $0 < p < p_1$. In this case, $Q_0(x) = 0$ has two positive roots $x = x_1^p$ and $x = x_2^p$. Let $y_i^p = F(x_i^p), i = 1, 2$. When $x_1^p < K \leqslant x_2^p$, $E_1(x_1^p, y_1^p)$ is a unique positive equilibrium. When $K > x_2^p$, $E_1(x_1^p, y_1^p)$ and $E_2(x_2^p, y_2^p)$ are two positive equilibria.

Case III: $p = p_1$. In this case, $Q_0(x) = 0$ has two identical positive roots $x_{E_1} = x_1^{p_1}$. Let $y_1^{p_1} = F(x_1^{p_1})$. If $K > x_1^{p_1}$, then $E_1(x_{E_1}, y_{E_1})$ is a unique positive equilibrium.

□

3.1.2. Stability of equilibria

For any equilibrium $\overline{E}(\overline{x}, \overline{y})$, the Jacobian matrix is

$$J_{\overline{E}} = \begin{pmatrix} P(\overline{x}, \overline{y}) + \overline{x}P_x(\overline{x}, \overline{y}) & \overline{x}P_y(\overline{x}, \overline{y}) \\ \overline{y}Q'(\overline{x}) & Q(\overline{x}) \end{pmatrix}$$

The corresponding characteristic equation is

$$|\lambda\overline{E} - J_{\overline{E}}| = \lambda^2 - p_{\overline{E}}\lambda + q_{\overline{E}} = 0,$$

where

$$p_{\overline{E}} \triangleq P(\overline{x}, \overline{y}) + \overline{x}P_x(\overline{x}, \overline{y}) + Q(\overline{x}),\ q_{\overline{E}} \triangleq P(\overline{x}, \overline{y})Q(\overline{x}) + \overline{x}P_x(\overline{x}, \overline{y})Q(\overline{x}) - \overline{xy}P_y(\overline{x}, \overline{y})Q'(\overline{x}).$$

Theorem 3.2. *$E_O(0, 0)$ is a saddle point and unstable. $E_K(K, 0)$ is a saddle point for Cases (A1-1)–(A1-3), and it is locally asymptotically stable for Cases (A1-4), (A2) and (A3). $E_1(x_1^p, y_1^p)$ is locally asymptotically stable for Cases (A1-1), (A1-3) and (A2-1), and unstable for Cases (A1-2), (A1-4) and (A2-2). E_2 is a saddle point and unstable for Case (A2).*

Proof of Theorem 3.2. Since $q_{E_O} = -rs < 0$, E_O is a saddle point. Given that $q_{E_K} = -rQ(K)$, and for Cases (A1-1)–(A1-3), $Q(K) > 0$; then, E_K is a saddle point. For Case (A1-4), (A2) and (A3), $Q(K) < 0$ and $p_{E_K} = Q(K) - r < 0$; then, E_K is locally asymptotically stable. When $K = x_2^p$, there is $Q(K) = 0$; in this case, E_K is a saddle-node.

For $\overline{E}(\overline{x}, \overline{y})$, we have

$$p_{\overline{E}} = -\frac{2rh_1\overline{x}}{k(1 + h_1\overline{x})}\left[\overline{x} - \frac{h_1K - 1}{2h_1}\right], q_{\overline{E}} = \frac{b\overline{x}^2\overline{y}Q_0'(\overline{x})}{(1 + h_1\overline{x})(1 + h\overline{x})}.$$

For Cases (A1-1), (A1-3) and (A2-1), there exist $q_{E_1} > 0$ and $p_{E_1} < 0$ due to $Q_0'(x_1^p) > 0$ and $K < 2x_1^p + 1/h_1$, which implies that $E_1(x_1^p, y_1^p)$ is locally asymptotically stable; for Cases (A1-2) and (A2-2), there is $p_{E_1} > 0$; then, $E_1(x_1^p, y_1^p)$ is unstable. For Case (A1-2), there is $\dot{y} \leq 0$ and $\dot{y} = 0$ if and only if $x = x_1^p$, so E_1 is unstable. For Case (A1-2), a limit cycle Γ_{LC} exists around E_1. Since $Q_0'(x_2^p) < 0$ for Case (A2), i.e., $q_{E_2} < 0$, $E_2(x_2^p, y_2^p)$ is a saddle point and unstable. □

3.2. Dynamics of the capture system (2.3)

For System (2.3), there are

$$\mathcal{M} = \{(x, y)|wx + (1 - w)y = H\},\ \mathcal{N} = \left\{(x, y)|\frac{w}{1 - q_1E}x + \frac{1 - w}{1 - q_2E}(y - \tau) = H\right\},$$

and we denote $k_{\mathcal{M}} \triangleq -w/(1 - w)$ and $K_{\mathcal{N}} \triangleq k_{\mathcal{M}}(1 - q_2E)/(1 - q_1E)$.

3.2.1. Periodic solution for $\tau = 0$

In this case, the system (2.2) has a subsystem (3.1) since $y \equiv 0$ if $y_0 = 0$

$$\begin{cases} \dfrac{dx}{dt} = rx\left(1 - \dfrac{x}{K}\right), & x \neq x_H, \\ \Delta x = -q_1Ex, & x = x_H, \end{cases} \tag{3.1}$$

where $w > 0$ and $x_H \triangleq Hw^{-1}$.

Denote $\overline{\xi}_0 = (1 - q_1E)x_H$ and

$$T \triangleq \frac{1}{r}\ln\left(\frac{K - (1 - q_1E)x_H}{(1 - q_1E)(K - x_H)}\right); \tag{3.2}$$

then, a periodic solution exists in the subsystem (3.1):

$$\overline{\xi}(t) = \frac{K(1 - q_1E)x_H \exp(r(t - (n - 1)T)}{(K - (1 - q_1E)x_H) + (1 - q_1E)x_H \exp(r(t - (n - 1)T)))}, (n - 1)T \leq t \leq nT.$$

Define

$$R_0 \triangleq (1 - q_2E)(1 - q_1E)^{\frac{s}{r}}\left(1 - \frac{(h - 1)Kq_1Ex_H}{((1 + h)K - (1 - q_1E)hx_H)(K - x_H)}\right)^{\frac{\mu bK}{r(1-h)}}\left(\frac{K - x_H}{K - (1 - q_1E)x_H}\right)^{\frac{s+Kp}{r}}.$$

Theorem 3.3. *For the case $w > 0$ and $\tau = 0$, if $H < wK$, there exists a periodic solution $\mathbf{z} = (\overline{\xi}(t), 0)$ in System* (2.3)*, and it is orbitally asymptotically stable when $R_0 < 1$.*

Proof of Theorem 3.3. The proof can be seen as Theorem 2 in [21, 45]; therefore, it is omitted here. □

3.2.2. Periodic solution for $\tau > 0$

The intersection point of $\mathcal{N}$ with the x-axis is denoted as $G(x_G, y_G)$. For $0 < \sigma < \tau$, select a point $Q \in \mathcal{N} \cap U(G, \sigma)$, where the trajectory $\mathbf{z}(t)$ with $\mathbf{z}(0) = Q$ intersects $\mathcal{M}$ at Q^-, and denote Q^+ as the phase point of Q^- after the pulse.

The trajectory of System (2.2) tangent to $\mathcal{N}$ is denoted by $\hat{\mathbf{z}}(t)$, and the tangent point is denoted by $A(x_A, y_A)$, i.e. $\mathrm{d}\hat{y}/\mathrm{d}\hat{x}|_A = k_{\mathcal{N}}$. If $\gamma_A(\hat{\mathbf{z}}) \cap \mathcal{M} \neq \emptyset$, let A^- be the first intersection point, and A^+ be the phase point of A^- after the pulse. If $\gamma_A(\hat{\mathbf{z}}) \cap \mathcal{M} = \emptyset$ or $\gamma_{A'}(\hat{\mathbf{z}}) \cap \mathcal{M} = \{A^-\}$ for some $A'(\neq A) \in \mathcal{N}$, then let $\tilde{\mathbf{z}}(t)$ be the trajectory tangent to $\mathcal{M}$, and the tangent point is denoted by F, i.e. $\mathrm{d}\tilde{y}/\mathrm{d}\tilde{x}\,|_F = k_{\mathcal{M}}$. Moreover, let $R_1(x_{R_1}, y_{R_1}) \in \mathcal{N}$ and $R_2(x_{R_2}, y_{R_2}) \in \mathcal{N}$ with $y_{R_2} < y_{R_1}$ such that $\gamma_{R_i}(\hat{\mathbf{z}}) \cap \mathcal{M} = \{F\}$ $(i = 1, 2)$. For Case (A1-2), if $\Gamma_{LC} \cap \mathcal{M} \neq \emptyset$, then denote $\Gamma_{LC} \cap \mathcal{M} = \{M_1, M_2\}$ with $y_{M_2} < y_{M_1}$. Similarly, if $\Gamma_{LC} \cap \mathcal{N} \neq \emptyset$, then denote $\Gamma_{LC} \cap \mathcal{N} = \{N_1, N_2\}$ with $y_{N_2} < y_{N_1}$.

Define $H_i \triangleq wx_i^p + (1 - w)y_i^p$ $(i = 1, 2)$ and

$$\overline{H}_K^p \triangleq \begin{cases} \max\{H|\{\pi(A, t)|t \geq 0\} \cap M \neq \emptyset\}, \text{for Cases } (A1\text{-}1), (A1\text{-}3), \\ \max\{H|\Gamma_{LC} \cap M \neq \emptyset\}, \text{for Case } (A1\text{-}2), \\ wK, \text{for Cases } (A1\text{-}4), (A3). \end{cases} \tag{3.3}$$

For Cases (A1) and (A3), we have

Theorem 3.4. *For System* (2.3)*, there exists an order-1 periodic solution for $w > 0$ and $H \leq \overline{H}_K^p$ in any case of (A1-1), (A1-3), (A1-4) and (A3). Moreover, for the case (A1-1) (or (A1-3)) and $H > \overline{H}_K^p$, an order-1 periodic solution exists if $x_{R_2} \leq (1 - q_1E)x_F$. For the case (A1-2), an order-1 periodic solution exists for $w > 0$ and $H \leq H_1$; while, for $H_1 < H \leq \overline{H}_K^p$, an order-1 periodic solution exists if $x_{N_2} \leq (1 - q_1E)x_{M_2}$.*

Proof of Theorem 3.4. In any case of (A1-1) or (A1-3) or (A1-4) or (A3), for $w > 0$ and $H \le \overline{H}^p_K$, any trajectory starting from $\mathcal{N}$ will intersect $\mathcal{M}$, as illustrated in Figure 1. For the point A, if $y_{A^+} = y_A$, then the orbit $\gamma_A(\mathbf{z})$ forms an order-1 periodic solution. Otherwise,

i) In the case of $y_{A^+} < y_A$, we have $f^{\mathrm{I}}_{\mathrm{SOR}}(A) = d_{A^+G} - d_{AG} < 0$. Since $f^{\mathrm{I}}_{\mathrm{SOR}}(Q) = d_{Q^+G} - d_{QG} > 0$, then $\exists S \in \overline{AQ}$ such that $f^{\mathrm{I}}_{\mathrm{SOR}}(S) = 0$, which means that the orbit $\gamma_S(\mathbf{z})$ forms an order-1 periodic solution, as illustrated in Figure 2 (a);

ii) In the case of $y_{A^+} > y_A$, we have $f^{\mathrm{I}}_{\mathrm{SOR}}(A) = d_{A^+G} - d_{AG} > 0$. The orbit $\gamma_{A^+}(\mathbf{z})$ intersects $\mathcal{M}$ at A^{+-}, and then it is pulsed to the point A^{++}. Since $y_{A^-} > y_{A^{+-}}$ and $y_{A^+} > y_{A^{++}}$, we have $f^{\mathrm{II}}_{\mathrm{SOR}}(A^+) = d_{A^{++}G} - d_{A^+G} < 0$. Next, according to the continuity of the solution, for $\epsilon = d_{AA^+}/2$, we can select a point $H \in \mathcal{N} \cap U(A, \epsilon)$, and there is $d_{H^-A^-} < \epsilon$. Then, by the impulse effects, there is $d_{H^+A^+} \le \max\{1 - q_1 E, 1 - q_2 E\}\epsilon < \epsilon$. Thus

$$\begin{aligned} f^{\mathrm{II}}_{\mathrm{SOR}}(H) &= d_{H^+G} - d_{HG} \\ &= d_{A^+G} - d_{H^+A^+} - d_{AG} - d_{AH}. \\ &= d_{A^+A} - (d_{H^+A^+} + d_{AH}) > 0. \end{aligned}$$

The continuity of $f^{\mathrm{II}}_{\mathrm{SOR}}$ implies that there exists $S \in \overline{HA^+}$ such that $f^{\mathrm{II}}_{\mathrm{SOR}}(S) = 0$, as illustrated in Figure 2(b).

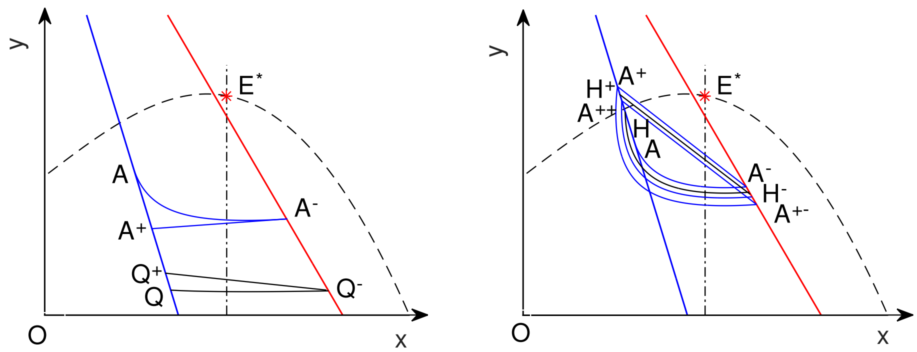

Figure 2. Schematic diagram of trajectory change in System (2.3) for Case (A1-1) (or (A1-3)) and $H < H^p_K$: (a) $y_{A^+} < y_A$; (b) $y_{A^+} > y_A$.

Moreover, for Case (A1-1) (or (A1-3)) and $H > \overline{H}^p_w$, if $x_{R_2} \le (1 - q_2 E)x_F$, then $f^{\mathrm{I}}_{\mathrm{SOR}}(R_2) = d_{F^+G} - d_{R_2G} \le 0$. Similar to Case I), there exists an order-1 periodic solution in system (2.3). While, for (A1-2), we can adopt a proof similar to (A1-1); hence, it is omitted. □

For Case (A2), two positive equilibria E_1 and E_2 exist simultaneously in System (2.2), where E_2 is a saddle point, E_K is locally asymptotically stable. Define

$$w^*_i \triangleq \frac{y^p_i}{K - x^p_i + y^p_i}, i = 1, 2.$$

For Case (A2-1), E_1 is locally asymptotically stable. For Case (A2-2), E_1 is unstable. Moreover, there exists $\overline{K} > \underline{K}$ and System (2.2) has a limit cycle Γ_{LC} for $\underline{K} < K < \overline{K}$. In this case, let $\overline{H} \triangleq$

$\max\{H|\Gamma_{LC} \cap \mathcal{M} \neq \emptyset\}$. For $H_1 < H \leq \overline{H}$, denote $\Gamma_{LC} \cap \mathcal{M} = \{D_1, D_2\}$ with $y_{D_1} \leq y_{D_2}$. Similarly, if $\Gamma_{LC} \cap \mathcal{N} \neq \emptyset$, denote $\Gamma_{LC} \cap \mathcal{N} = \{B_1, B_2\}$ with $y_{B_1} \leq y_{B_2}$. For $K \geq \overline{K}$, E_K is globally asymptotically stable.

Since E_2 is a saddle point, let Γ_{SM} and Γ_{USM} respectively represent the stable and unstable manifolds that pass through E_2 below the isoline $\dot{x} = 0$. For $H_1 < H \leq H_2$, denote $\Gamma_{\text{SM}} \cap \mathcal{M} = \{D\}$. If $\Gamma_{\text{SM}} \cap \mathcal{N} \neq \emptyset$, then denote B as the intersection point with a smaller y label. Otherwise, let B be a point on $\mathcal{N}$ with $y_B = (1 - q_2E)y_D + \tau$. For $H_2 < H \leq wK$, denote $\Gamma_{\text{USM}} \cap \mathcal{M} = \{D\}$, and $\Gamma_{\text{SM}} \cap \mathcal{N} = \{B\}$.

Theorem 3.5. *For Case (A2), there exists an order-1 periodic solution in System* (2.3) *if one of the conditions holds: 1)* $0 < w \leq w_1^*$ *and* $H \leq wK$*; 2)* $w_1^* < w \leq 1$ *and* $H \leq H_1$*; 3)* $w_1^* < w \leq w_2^*$*,* $H_1 < H \leq wK$ *and* $y_{B_1} \geq (1 - q_2E)y_{D_1} + \tau$*; 4)* $w_2^* < w \leq 1$*,* $H_2 < H \leq wK$ *and* $y_B \geq (1 - q_2E)y_D + \tau$*.*

Proof of Theorem 3.5. It can be easily verified that for any case of 1) $0 < w \leq w^*$ and $H \leq wK$ or 2) $w^* < w \leq 1$ and $H \leq H_1$, any trajectory starting from $\mathcal{N}$ will intersect $\mathcal{M}$; then, using a proof similar to Theorem 3.4, we can prove that there exists an order-1 periodic solution. While, for 3), $w_1^* < w \leq w_2^*$ and $H_1 < H \leq H_2$, if $y_{B_1} \geq (1 - q_2E)y_{D_1} + \tau$, any trajectory starting from $\overline{B_2G} \subset \mathcal{N}$ will intersects $\mathcal{M}$; similarly, we can prove that there exists an order-1 periodic solution. Case 4) is similar to Case 3) and thereby omitted. □

Let $\tilde{\mathbf{z}} = (\tilde{\xi}(t), \tilde{\eta}(t))$, $0 \leq t \leq T$ be the order-1 P.S.. Denote $\xi_1 = \tilde{\xi}(T), \eta_1 = \tilde{\eta}(T), \xi_0 = (1 - q_1E)\,\xi_1$, $\eta_0 = (1 - q_2E)\,\eta_1 + \tau$, $f_1^0 = f_1(\xi_0, \eta_0), f_1^1 = f_1(\xi_1, \eta_1), f_2^0 = f_2(\xi_0, \eta_0)$ and $f_2^1 = f_2(\xi_1, \eta_1)$. Then, we have the following theorem.

Theorem 3.6. *The order-1 periodic solution* $\tilde{\mathbf{z}} = (\tilde{\xi}(t), \tilde{\eta}(t))$ *is orbitally asymptotically stable if*

$$\int_0^T \left(\frac{bh_1\tilde{\xi}(t)\tilde{\eta}(t)}{\left(1 + h_1\tilde{\xi}(t)\right)^2} - \frac{r\tilde{\xi}(t)}{K} \right) dt < \ln\left(\left| \frac{\xi_0\eta_0}{\xi_1\eta_1} \cdot \frac{wf_1^1 + (1 - w)f_2^1}{(1 - q_2E)wf_1^0 + (1 - q_1E)(1 - w)f_2^0} \right| \right). \tag{3.4}$$

Proof of Theorem 3.6. From Model (2.3), we have

$$f_1(x, y) = rx\left(1 - \frac{x}{K}\right) - \frac{bxy}{1 + h_1x}, f_2(x, y) = \frac{\mu bxy}{1 + hx} - sy - pxy,$$
$$\chi(x, y) = wx + (1 - w)y - H, I_1(x, y) = -q_1Ex, I_2(x, y) = -q_2Ey + \tau.$$

Then we have

$$\frac{\partial f_1}{\partial x} = r - \frac{2rx}{K} - \frac{by}{(1 + h_1x)^2}, \frac{\partial f_2}{\partial y} = \frac{\mu bx}{1 + hx} - s - px,$$
$$\frac{\partial I_1}{\partial x} = -q_1E, \frac{\partial I_1}{\partial y} = 0, \frac{\partial I_2}{\partial x} = 0, \frac{\partial I_2}{\partial y} = -q_2E, \frac{\partial \chi}{\partial x} = w, \frac{\partial \chi}{\partial y} = 1 - w.$$

In addition,

$$\Delta_1 = \frac{f_1^+\left(\frac{\partial I_2}{\partial y}\frac{\partial \chi}{\partial x} - \frac{\partial I_2}{\partial x}\frac{\partial \chi}{\partial y} + \frac{\partial \chi}{\partial x}\right) + f_2^+\left(\frac{\partial I_1}{\partial x}\frac{\partial \chi}{\partial y} - \frac{\partial I_1}{\partial y}\frac{\partial \chi}{\partial x} + \frac{\partial \chi}{\partial y}\right)}{f_1\frac{\partial \chi}{\partial x} + f_2\frac{\partial \chi}{\partial y}}$$
$$= \frac{(1 - q_2E)wf_1^0 + (1 - w)(1 - q_1E)f_2^0}{wf_1^1 + (1 - w)f_2^1},$$

$$\exp\left(\int_0^T\left(\frac{\partial f_1}{\partial x}+\frac{\partial f_2}{\partial y}\right)_{(\tilde{\xi}(t),\tilde{\eta}(t))}\mathrm{d}t\right)=\frac{\xi_1\eta_1}{\xi_0\eta_0}\exp\int_0^T\left(\frac{bh_1\tilde{\xi}\tilde{\eta}}{(1+bh\tilde{\xi})^2}-\frac{r\tilde{\xi}}{K}\right)\mathrm{d}t.$$

Thus,

$$\mu_1=\Delta_1\exp\left(\int_0^T\left(\frac{\partial f_1}{\partial x}+\frac{\partial f_2}{\partial y}\right)_{(\tilde{\xi}(t),\tilde{\eta}(t))}\mathrm{d}t\right)=\Delta_1\frac{\xi_1\eta_1}{\xi_0\eta_0}\exp\int_0^T\left(\frac{bh_1\tilde{\xi}\tilde{\eta}}{(1+bh\tilde{\xi})^2}-\frac{r\tilde{\xi}}{K}\right)\mathrm{d}t.$$

Therefore, $|\mu_1|<1$ if and only if (3.4) holds; then, by Lemma 2.1, the order-1 periodic solution $\tilde{\mathbf{z}}=(\tilde{\xi}(t),\tilde{\eta}(t))$ is orbitally asymptotically stable. □

Theorem 3.7. *For the case (A1-1) (or (A1-3)) and $H\le\overline{H}_K^p$, the order-1 periodic solution $\mathbf{z}=(\tilde{\xi}(t),\tilde{\eta}(t))$ is orbitally asymptotically stable and globally attractive if $y_{A^+}<y_A$.*

Proof of Theorem 3.7. According to Theorems 4 and 5, when $H\le\overline{H}_K^p$, there exists an order-1 P.S. in system (2.3). If $y_{A^+}<y_A$, then $L\in\overline{AQ}$, which means that for any $S\in N$, $f^{\mathrm{I}}_{\text{SOR}}(S)<0$ with $y_S>y_L$, $f^{\mathrm{I}}_{\text{SOR}}(S)>0$ with $y_S<y_L$ and $f^{\mathrm{I}}_{\text{SOR}}(S)=0$ if and only if $S=L$. Thus, for any $S_0^+\in\overline{AL}\subset N$, there exists a sequence $\{S_k^+\}(k=0,1,2,\cdots)$ satisfying $y_{S_{k+1}^+}=y_{S_k^+}+f^{\mathrm{I}}_{\text{SOR}}(S_k^+)$. If $S_0^+\in\overline{AL}$, $\{S_k^+\}$ is monotonically decreasing. Moreover, y_L is the lower limit. If $S_0^+\in\overline{LQ}$, $\{S_k^+\}$ is monotonically increasing, and y_L is the upper limit. Thus $y_{S_k^+}\to y_{S'}(k\to\infty)$. Therefore,

$$f^{\mathrm{I}}_{\text{SOR}}(S')=f^{\mathrm{I}}_{sor}(\lim_{k\to\infty}S_k^+)=\lim_{k\to\infty}f^{\mathrm{I}}_{\text{SOR}}(S_k^+)=\lim_{k\to\infty}(y_{S_{k+1}^+}-y_{S_k^+})=0.$$

Moreover $f^{\mathrm{I}}_{\text{SOR}}(S)=0$; then, we have $S'=S$, and the orbit from any point $S_0^+\subset\mathcal{N}$ will approach $\mathbf{z}=(\tilde{\xi}(t),\tilde{\eta}(t))$, which means that $\mathbf{z}=(\tilde{\xi}(t),\tilde{\eta}(t))$ is globally attractive. □

Next, we discuss the order-2 periodic solution. For a given point $S(x_S,y_S)$ on N with $0\le y_S\le\overline{y}\triangleq(1-q_2E)H/(1-w)+\tau$, when $y_S\le y_A$, there is $\psi_N(y_S)=(1-q_2E)\pi(S,T_S)+\tau$. While for $y_S>y_A$, there exists a unique $S'\in N$ with $y_{S'}\in(0,y_A)$ and $\hat{T}_z$ such that $y_{S'}=\pi(S,\hat{T}_S)$. Then $\psi_N(y_S)=(1-q_2E)\pi(S,T_{S'})+\tau$. For the above summary, there is

$$\psi_N(y_S)=\begin{cases}(1-q_2E)\pi(S,T_S)+\tau, & y_S\le y_A\\ (1-q_2E)\pi(S,T_{S'})+\tau, & y_S>y_A\end{cases}\tag{3.5}$$

Property 3.1. *For Case (A1) and $H\le\overline{H}_K^p$, the Poincaré map ψ_N defined by* (3.5) *has the following characteristics: 1) ψ_N is continuous on* $[0,\overline{y}]$. *Moreover, ψ_N increases and then decreases, and it reaches a maximum at $y=y_A$; 2) ψ_N is continuously differentiable on* $[y_A,\overline{y}]$.

For Case $(A1)$ and $H\le H_K^p$, if $\psi_N(y_A)<y_A$, the order-1 periodic solution of System (2.3) is orbitally asymptotically stable and globally attractive (Theorem 3.7); in this case, there does not exist an order-n $(n\ge2)$ periodic solution. For the case $\psi_N(y_A)>y_A$, there exists a unique $y_{L_2}\in[y_A,\psi_N(y_A)]$ such that $\psi_N(y_{L_2})=y_{L_2}$. Let $y_{L_1}\in[0,y_A]$ such that $\psi_N(y_{L_1})=y_{L_2}$. Then $\psi_N^2(y_{L_1})=\psi_N(y_{L_2})=y_{L_2}$. Meanwhile, let $y_{N_1}\in[0,y_A]$ and $y_{N_2}\in[y_{L_2},\overline{y}]$ such that $\psi_N(y_{N_1})=\psi_N(y_{N_2})=y_A$.

Theorem 3.8. *For $w>0$, $H\le\overline{H}_K^p$ and $\psi_N(y_A)>y_A$, if i) $\psi_N^2(y_A)<y_A$ or ii) $\psi_N^2(y_A)>y_A$ and $\mu_1>1$ holds, then there exists an order-2 periodic solution in System* (2.3).

Proof of Theorem 3.8. Because $\psi_N(y_{N_1})=\psi_N(y_{N_2})=y_A$, obviously, $\psi_N^2(y_1)=\psi_N^2(y_2)=\psi_N(y_A)$. Then, ψ_N^2 is increasing on $[0,y_{N_1}]$ and $[y_A,y_{N_2}]$ and ψ_N^2 is decreasing on $[y_{N_1},y_A]$ and $[y_{N_2},\overline{y}]$. Since $\psi_N^2(y_{N_1})=\psi_N(y_A)>y_A>y_{N_1}$, there is $\psi_N^2(y_{N_1})>y_{N_1}$.

i) If $\psi_N^2(y_A) < y_A$, then there is $\psi_N(y_A) > y_{N_2}$. As $\psi_N(y_A) = \psi_N^2(y_{N_2})$, there is $\psi_N^2(y_{N_2}) > y_{N_2}$, which also implies that $\psi_N^2(\psi_N(y_A)) < \psi_N(y_A)$. Thus there exist $y_{M_1} \in [y_{N_1}, y_A]$ and $y_{M_2} \in [y_{N_2}, \psi_N(y_A)]$ such that $\psi_N^2(y_{M_1}) = y_{M_1}, \psi_N^2(y_{M_2}) = y_{M_2}$. And there is $\psi_N(y_{M_2}) = y_{M_1}, \psi_N(y_{M_1}) = y_{M_2}$.

ii) If $\psi_N^2(y_A) > y_A$, there is $\psi_N(y_A) < y_{N_2}$, i.e. $\psi_N^2(y_{N_2}) < y_{N_2}$. For any $y \in [y_A, \psi_N(y_A)]$, we have $y_A < \psi_N(y) < \psi_N(y_A)$. Next, it discusses the property of ψ_N on $[y_A, \psi_N(y_A)]$. Let $y_0 = y_A$; then, $y_1 = \psi_N(y_0) = \psi_N(y_A) > y_0, y_2 = \psi_N(y_1) = \psi_N^2(y_0) > y_0$ and $y_3 = \psi_N(y_2) < \psi_N(y_0) = y_1$. A sequence $\{y_n\}$ is obtained under ψ_N, where $y_0 < y_2 < y_4 < \cdots < y_{L_2} < \cdots < y_5 < y_3 < y_1$. Denote $y_{M_1} = \lim_{n\to\infty} y_{2n}$ and $y_{M_1} = \lim_{n\to\infty} y_{2n+1}$. It is obvious that $y_{M_1} \le y_{L_2} \le y_{M_2}$. Since $\mu_1 > 1$, $y_{M_1} < y_{L_2} < y_{M_2}$. Besides $\psi_N(y_{M_2}) = y_{M_1} and \psi_N(y_{M_1}) = y_{M_2}$, so $\mu_2 < 1$, i.e., the order-2 periodic solution is orbitally asymptotically stable.

□

3.3. Fishing process optimization

In order to realize the sustainability of fishery resources and maximize economic benefits, it is necessary to consider the problem of harvest optimization. In Model (2.3), let $H = wl + (1 - w)ml$, where $m \triangleq y_1^p/x_1^p$, and the weight w and harvest density l are the decision variables. Besides, we assume that E and τ are also linearly dependent on the decision variables w and l, i.e.

$$
\begin{aligned}
E(l) &= E_{\min} + (E_{\max} - E_{\min})\frac{l - l_1}{l_2 - l_1},\\
\tau(w, l) &= w\left[\tau_1 + (\tau_2 - \tau_1)\frac{l - l_1}{l_2 - l_1}\right],
\end{aligned}
\tag{3.6}
$$

where l_1 and l_2 are, respectively, the lower and upper limits of the harvest level, $E_{\min}$ and $E_{\max}$ respectively represent the minimum and maximum harvest effort and τ_1 and τ_2 respectively represent the minimum and maximum quantities of released predator populations. Let c_1 be the unit sale revenue of prey species, c_2 represent that of predator species, c_3 denote the unit price of harvesting and c_4 be the feeding predator unit cost. In general, c_3 and c_4 are fixed, and c_1/c_2 varies with season and market demand; also, denote $\sigma \triangleq c_2/c_1$. Therefore, the total revenue can be expressed as $H_{benefit}(w, l) = c_1 q_1 E(l)\xi(T(w, l)) + c_2 q_2 E(l)\eta(T(w, l)) - c_3 E(l) - c_4 T(l)$. The objective is to find the maximum of $P_{benefit}(w, l)$, which can be described as follows:

$$
\begin{aligned}
&\max P_{benefit} = \frac{H_{benefit}(w, l)}{T(w, l)}\\
&\text{such that } \ l_1 \le l \le l_2, 0 \le w \le 1.
\end{aligned}
\tag{3.7}
$$

The optimal control level l^*, w^* can be obtained by solving the optimization model (3.7). Accordingly, it is possible to determine the release amount $\tau^* = \tau(l^*, w^*)$, the optimal capture effort $E^* = E(l^*, w^*)$, and the optimal capture period $T^* = T(l^*, w^*)$.

4. Computer simulation verification

We will verify the main results through numerical simulations. For System (2.2), we set the model parameters as follows $r = 2$, $b = 20\% = 0.2$, $\mu = 10\% = 0.1$, $h_1 = 0.01$, $h_2 = 0.3$, $s = 14\% = 0.14$. Then there is $p_1 = 0.0018$.

4.1. Theory verification

4.1.1. Verification of Theorem 3.1 and Theorem 3.2

First, for K=100, how the anti-predator rate p affects the dynamics of the system (2.2) is presented in Figure 3. When $p = 0.0015$, two positive equilibria exist in the system; when $p = 0.0018$, a unique positive equilibrium exists; and, when $p = 0.02$, there is no positive equilibrium. It is clear that the anti-predator factor has a certain effect on the number of equilibria; with the increase of the anti-predator factor, the number of positive equilibria gradually decreases.

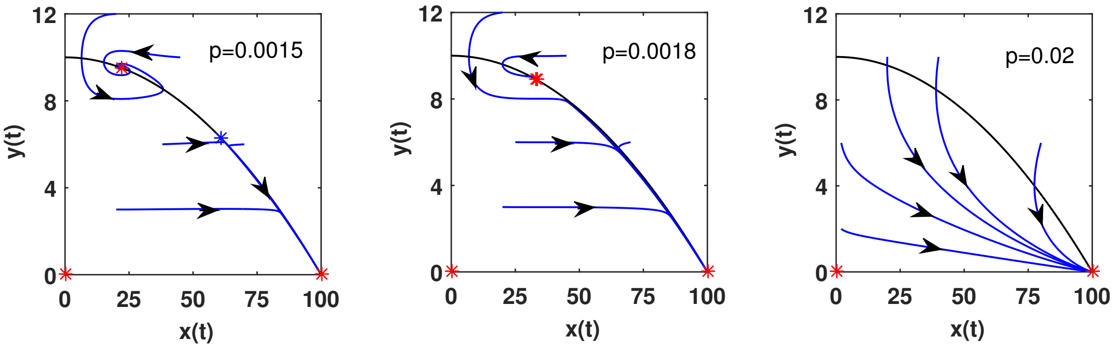

Figure 3. Effect of anti-predator rate p on the dynamics of the system (2.2).

Next, for $p = 0.0015$, how the environmental capacity K affects the dynamics of the system (2.2) is shown in Figure 4. For $K = 100$, E_1 is locally asymptotically stable, and for $K = 150$, E_1 is unstable; and, a limit cycle exists surrounding E_1; while, for $K = 200$, E_K is globally asymptotically stable.

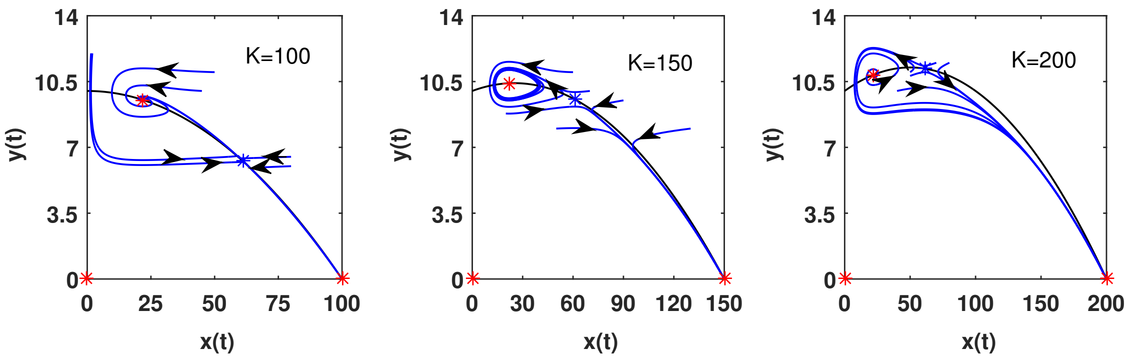

Figure 4. Effect of environmental capacity K on the dynamics of the system (2.2).

Next, we will verify the main results by changing the capture level H. The control parameters were set as $w = 0.2$, $\tau = 0.5$, $E = 1$, $q_1 = 0.5$ and $q_2 = 0.2$.

4.1.2. Verification of Theorem 3.4

Case I: $H \le \min\{H_1, wK\}$
Here we consider three subcases:

i) $p = 0$ and $K = 100$. Then a unique positive equilibrium $E_1(13.73, 9.81)$ exists in System (2.2). Since $H_1 = 10.5944$, for $H = 10$, there exists an order-1 periodic solution; its period is about

$T = 0.74$, as shown in Figure 5-4.

ii) $p = 0.0015$ and $K = 50$. Then at the positive equilibrium $E_1(21.8584, 6.8586)$, there is $H_1 = 9.86$. For $H = 9 < H_1$, there exists an order-1 periodic solution; its period is about $T = 1.35$, as illustrated in Figure 5-5.

iii) $p = 0.0018$ and $K = 100$. Then at the equilibrium $E_1(33.33, 8.89)$, there is $H_1 = 13.78$. For $H = 13 < H_1 = 13.78$, an order-1 periodic solution with the period $T = 0.84$ exists, as depicted in Figure 5-6.

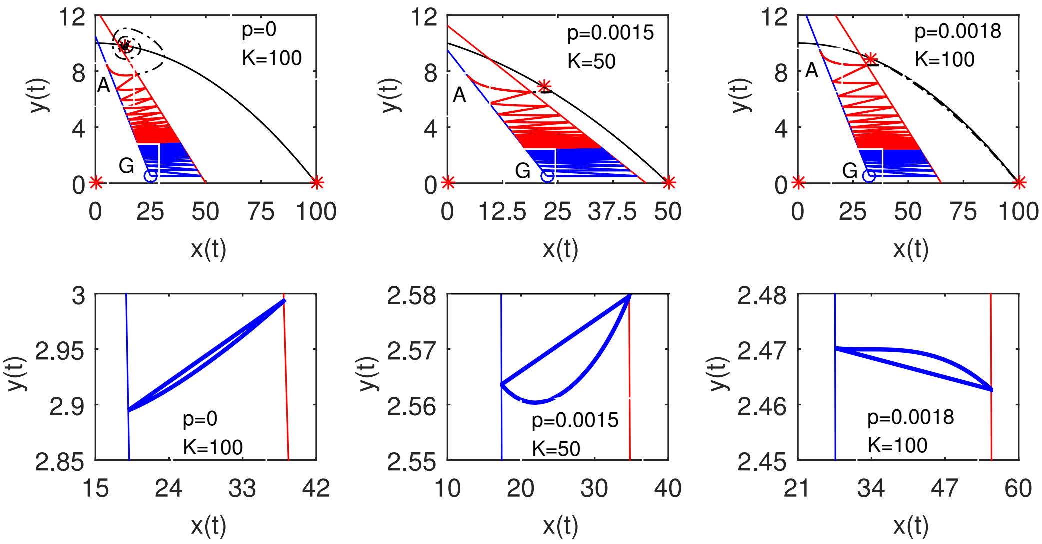

Figure 5. Diagram of trajectory tendency of the system (2.3) and presentation of the order-1 periodic solution with $H \le \min\{H_1, wK\}$ for different p and K in case $(A1)$.

Case II: $H_1 < H < H_2$

In this case, the order-1 periodic solution exists conditionally. For $p = 0$, $K = 100$ and $H = 13$, since $x_{R_2} \ge (1 - q_1E)x_F$ holds for a given q_1, q_2 and τ (Figure 6-1), an order-1 periodic solution exists (Figure 6-4); its period is about $T = 0.96$. It should be pointed out that the inequality is dependent on the values of q_1, q_2 and τ; once the inequality is reversed, all trajectories will go forward to E_1 after several pulses. For $p = 0.0015$, $K = 50$ and $H = 10$, System (2.3) also has an order-1 periodic solution with the period $T = 2.37$ (Figure 6-5) since $x_{R_2} \ge (1 - q_1E)x_F$ holds (Figure 6-2). For $p = 0.0018$, $K = 100$ and $H = 16$, since $x_B \ge (1 - q_1E)x_D$ holds for a given q_1, q_2 and τ (Figure 6-3), an order-1 periodic solution exists (Figure 6-6); its period is about $T = 1.144$.

4.1.3. Verification of Theorem 3.5

For Case $A2$, we assume that $p = 0.0015$; then, $x_1^p = 21.86$, $x_2^p = 61$ and $\underline{K} = 143.7$. Diagrams of the trajectory tendency of the System (2.3) for different values of K and H are illustrated in Figure 7.

For $K = 100$, $E_1(21.86, 9.52)$ is locally asymptotically stable. Since $H_1 = 12$, $H_2 = 17.2$ and $wK = 20$, for $H = 11$, the order-1 periodic solution exists unconditionally (Figure 7-1); for $H = 14$ and $H = 18$, when $y_B \ge (1 - q_2E)y_D + \tau$ holds, the existence of the order-1 periodic solution is guaranteed

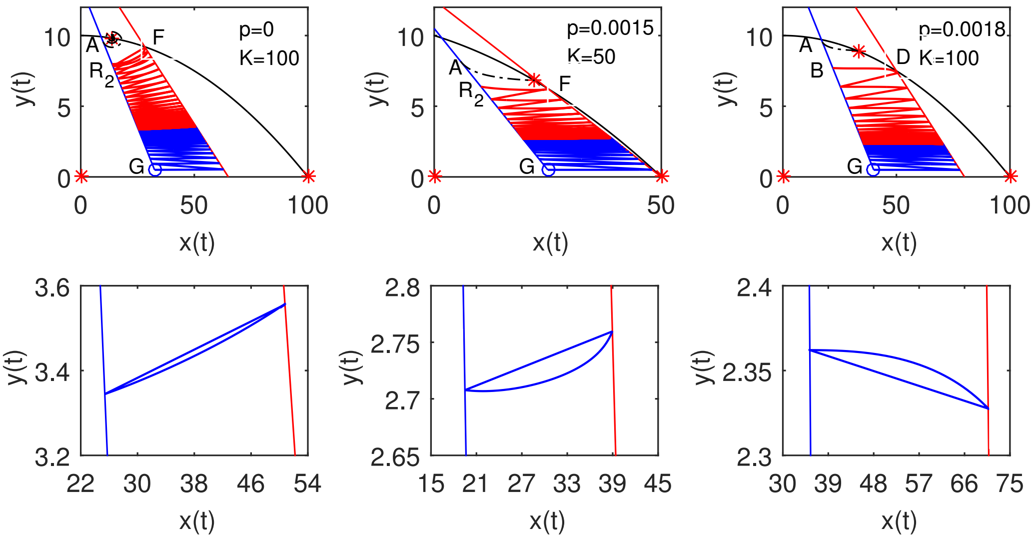

Figure 6. Diagram of trajectory tendency and order-1 periodic solution of system (2.3) with $H_1 < H < H_2$ for different values of p and K in Case $A1$.

(Figure 7-4 and Figure 7-7). For $K = 150 > \underline{K}$, $E_1(21.86, 10.4)$ is unstable and a limit cycle exists. In this case, $H_1 = 12.6$, $H_2 = 19.8$ and $wK = 30$. Similarly, for $H = 12$, the order-1 periodic solution exists unconditionally (Figure 7-2)), while for $H = 17$ and $H = 22$, when $y_B \geq (1-q_2E)y_D+\tau$ holds, the existence of the order-1 periodic solution is guaranteed (Figure 7-5 and Figure 7-8). For $K = 200 > \overline{K}$, $E_1(21.86, 10.4)$ is unstable and E_K is globally asymptotically stable. In this case, $H_1 = 13.1$, $H_2 = 21$ and $wK = 40$. Similarly, for $H = 13$, the order-1 periodic solution exists unconditionally (Figure 7-3); while, for $H = 19$ and $H = 25$, when $y_B \geq (1 - q_2E)y_D + \tau$ holds, the existence of the order-1 periodic solution is guaranteed (Figure 7-6 and Figure 7-9).

4.1.4. Verification of Theorem 3.8

For Case ($A2$), when $\underline{K} < K < \overline{K}$, E_1 is unstable and a limit cycle Γ_{LC} exists. For $H_1 < H \leq \overline{H}$ and a smaller τ with $y_B \geq (1-q_2E)y_D+\tau$, there exists an order-1 periodic solution (Theorem 3.5, Figure 7-5). Notice that $y_B \geq (1 - q_2E)y_D + \tau$ is just a sufficient condition to ensure that there is a periodic solution. In fact, as long as $y_{B_1} \geq (1-q_2E)y_{D_1}+\tau$, for example, $\tau = 1.74$, the order-1 periodic solution will exist (Figure 8-1) for $p = 0.0015$, $K = 150$ and $H = 15$. For a bigger τ, for example, $\tau = 2.1$ and $\tau = 2.2$, there may also exist an order-1 periodic solution (Figure 8-2, 8-3), but existence is not guaranteed. From Figure 8-2, it is observed that even if an order-1 periodic solution exists, its shape has changed. Figure 8-3 presents an order-2 periodic solution. The existence of an order-2 periodic solution implies the existence of an order-1 periodic solution, but in this case, the order-1 periodic solution is unstable.

The dynamics of System (2.3) depends on the control parameters w, q_1 and q_2. Next, we consider another set of control parameters: $w = 0.6$, $q_1 = 0.6$ and $q_2 = 0.4$. For $p = 0$ and $K = 150$, there is $K > \underline{K} = 127$; then, E_K is unstable, $E_1(13.72, 10.33)$ is unstable and a limit cycle exists. We have $H = 18.55 > H_1 = 12.37$. Presentation of the order-m periodic solution of System (2.3) for $p = 0$, $K = 150$, $H = 18.55$ and different values of τ is shown in Figure 9. For $\tau = 4.1$, System (2.3) has an

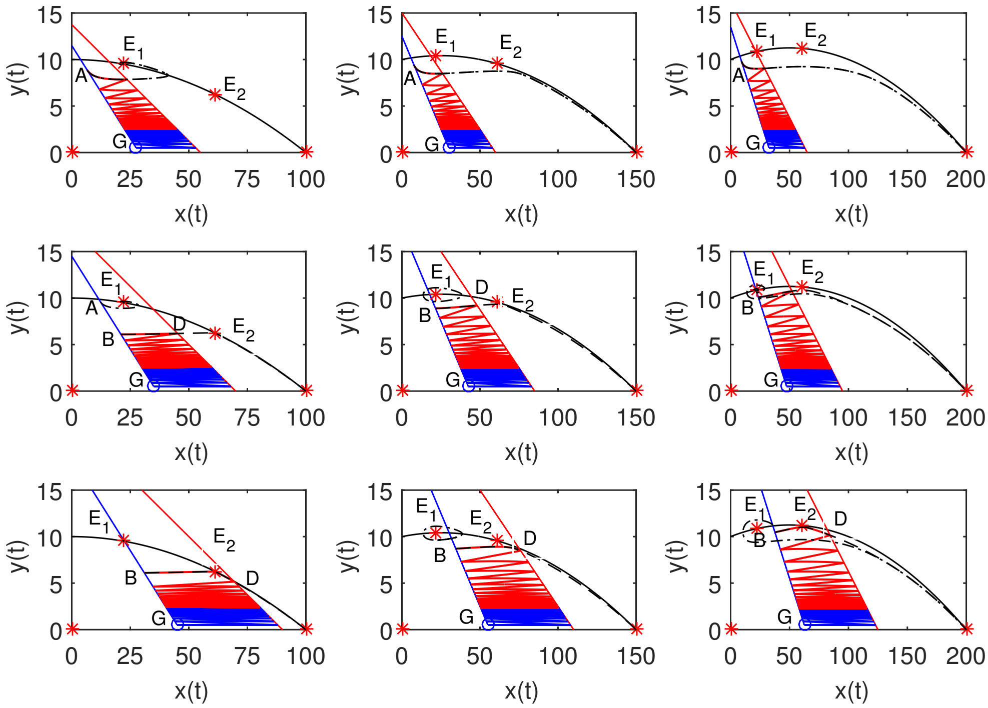

Figure 7. Diagram of the trajectory tendency of the System (2.3) for different values of K in Case $A2$: 1) $H < H_1$; 2) $H_1 < H < H_2$; 3)$H_2 < H < wK$.

order-2 periodic solution, as depicted in Figure 9-1. In this case, the order-1 periodic solution exists but is unstable. For $\tau = 4$, there exists an order-3 periodic solution (Figure 9-2) and for $\tau = 3.95$, System (2.3) has an order-4 periodic solution (Figure 9-3). The existence of an order-m periodic solution ($m \geq 3$) would also lead System (2.3) to chaos [42, 50].

4.2. Numerical optimization

Let $K = 100$, $E_1 = 40\%$, $E_2 = 100\%$, $\tau_1 = 0.5$ and $\tau_2 = 2$, and the other model parameters are the same as in the above simulations. Here, we consider two scenarios: 1) without anti-predator behavior, i.e., $p = 0$; 2) with anti-predator behavior, i.e., $p = 0.0015$. Besides, it is assumed that $l_1 = 20\% x_{E_1}$, $l_2 = 90\% x_{E_1}$, $c_1 = 5$, $c_3 = 30$ and $c_4 = 5$. For $p = 0$ and $\sigma = 20,\ 30$, the dependence of T and $P_{benefit}$ on w and l are presented in Figure 10. When $\sigma = 20$, the unit benefit $P_{benefit}$ achieves its maximum at $w^* = 0.1$ and $l^* = 0.69 x_{E_1}$. When $\sigma = 30$, $P_{benifit}$ achieves its maximum at $w^* = 1$ and $l^* = 0.34 x_{E_1}$.

For $p = 0.0015$, E_K is locally asymptotically stable. It is assumed that $0.1 \leq w \leq 1$. For $\sigma = 20,\ 30$, the dependence of T and $P_{benefit}$ on w and l are presented in Figure 11. For $\sigma = 20$, the unit benefit $P_{benefit}$ achieves its maximum at $w^* = 0.1$ and $l^* = 0.69 x_{E_1}$. For $\sigma = 30$, $P_{benifit}$ achieves its maximum at $w^* = 1$ and $l^* = 0.34 x_{E_1}$.

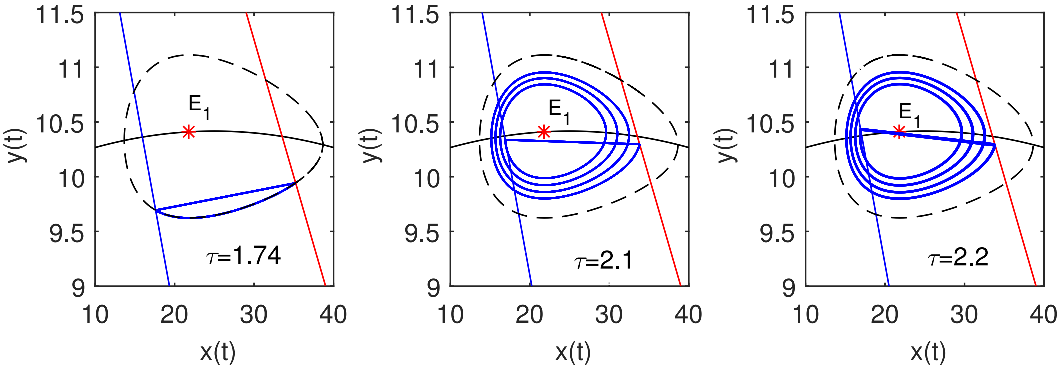

Figure 8. Presentation of the order-1 periodic solution for $p = 0.0015$, $K = 150$, $H = 15$ and different values of τ in Case $A2$.

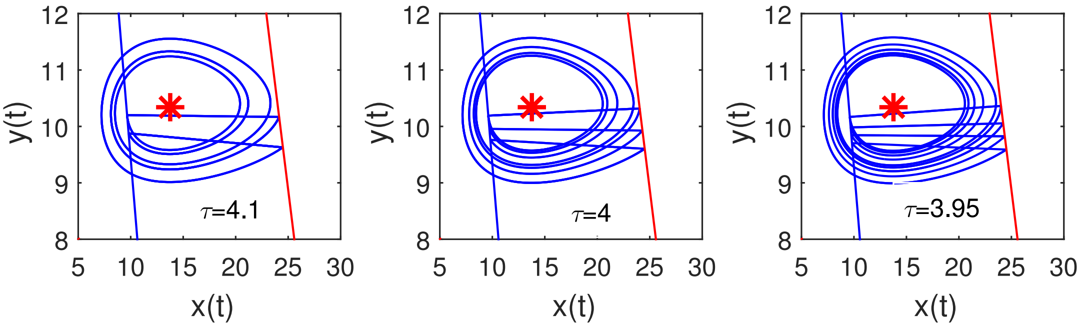

Figure 9. Presentation of the order-m periodic solution ($m = 2, 3, 4$) for $p = 0$, $K = 150$, $H = 18.55$ and different values of τ in case $A2$.

5. Summary and discussion

This work presented a fishery predator-prey model with anti-predator behavior and analyzed the dynamics of the model in detail. Besides, it introduced a weighted fishing strategy into the system and established a fishery capture model (2.2). It analyzed the dynamics of the model and showed that the anti-predation intensity affects the number of equilibria, that is, with the increase of anti-predation intensity, the number of equilibria will decrease (Figure 3). Moreover, it showed that, for a fixed anti-predator factor, the carrying capacity K has certain impact on the stability of the equilibria (Figure 4).

It also discussed the dynamic behavior of the capture model (2.3) according to different levels of anti-predation factors. The results showed that an order-1 periodic solution always exists when $H \le H_1$, no matter how strong the anti-predator factor (Figure 5 and Figure 7). For $H_1 < H \le H_2$, there is a constraint that ensures the existence of an order-1 periodic solution (Figure 6 and Figure 7). Moreover, for $0 \le p < p_1$ and $\underline{K} < K < \overline{K}$, System (2.3) presents an order-m periodic solution ($m \ge 2$) for certain values of τ (Figure 8 and Figure 9). However, it is difficult and challenging to prove the existence of an order-m periodic solution ($m > 2$), which will be our next study.

In the numerical optimization, it was shown that the benefits from fishing processes are dependent on the unit sales price of prey and predators, as well as on the harvest unit cost. For given values of

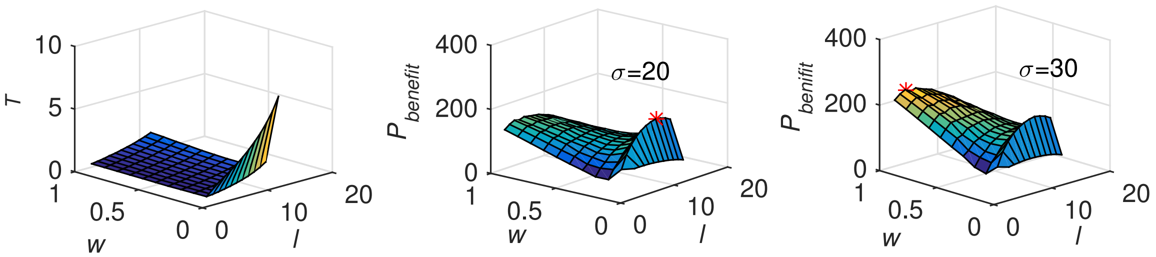

Figure 10. Dependence of T and $P_{benefit}$ on w and l for $p = 0$ and $K = 100$.

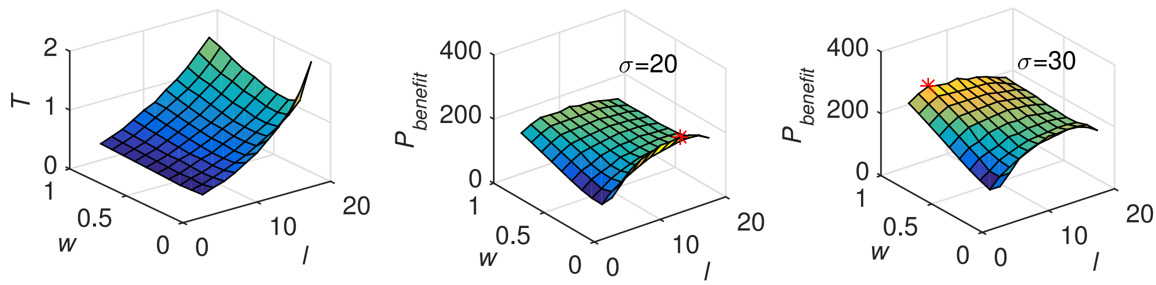

Figure 11. Dependence of T and $P_{benefit}$ on w and l for $p = 0.0015$ and $K = 100$.

c_1, c_3 and c_4, the unit benefit may achieve the maximum at different pairs of (l^*, w^*) for different values of σ (Figure 10 and Figure 11). This also indicates that we can determine the optimal capture strategy (E^*, τ^* and T^*) based on the selling prices of predators and prey, and then carry out fishing activities.

Funding

The research was supported by the Fundamental Research Funds for the Central Universities (No. DUT21LAB125).

Data availability statement

The data used to support the findings of this study are available from the corresponding author upon request.

Conflicts of interest

The authors declare that they have no known competing financial interests or personal relationships that could have appeared to influence the work reported in this paper.

References

1. Y. Choh, M. Ignacio, M. W. Sabelis, A. Janssen, Predator-prey role reversals, juvenile experience and adult antipredator behaviour, *Sci. Rep.*, **2** (2012), 728. https://doi.org/10.1038/srep00728

2. Z. Hoover, M. Ferrari, D. P. Chivers, The effects of sub-lethal salinity concentrations on the anti-predator responses of fathead minnows, *Chemosphere*, **90** (2013), 1047–1052. https://doi.org/10.1016/j.chemosphere.2012.08.051

3. C. M. O'Connor, A. R. Reddon, A. Odetunde, Social cichlid fish change behaviour in response to a visual predator stimulus, but not the odour of damaged conspecifics, *Behav Processes*, **121** (2015), 21–29. https://doi.org/10.1016/j.beproc.2015.10.002

4. A. Landeira-Dabarca, J. Nslund, J. I. Johnsson, Cue recognition and behavioural responses in the three-spined stickleback (Gasterosteus aculeatus) under risk of fish predation, *Acta Ethol.*, **22** (2019), 209—221. https://doi.org/10.1007/s10211-019-00324-8

5. P. Kłosiński, J. Kobak, M. Augustyniak, P. Pawlak, L. Jermacz, M. Poznańska-Kakareko, et al, Behavioural responses to con-and heterospecific alarm cues by an alien and a coexisting native fish, *Hydrobiologia*, **849** (2022), 985–1000. https://doi.org/10.1007/s10750-021-04761-0

6. T. Yokota, M. Machida, H. Takeuchi, S. Masuma, R. Masuda, N. Arai, Anti-predatory performance in hatchery-reared red tilefish (Branchiostegus japonicus) and behavioral characteristics of two predators: Acoustic telemetry, video observation and predation trials, *Aquaculture*, **319** (2011), 290–297. https://doi.org/10.1016/j.aquaculture.2011.07.010

7. B. Tang, Y. N. Xiao, Bifurcation analysis of a predator-prey model with anti-predator behaviour, *Chaos Soliton Fract*, **70** (2015), 58–68. https://doi.org/10.1016/j.chaos.2014.11.008

8. X. D. Sun, Y. P. Li, Y. N. Xiao, A Predator-Prey Model with Prey Population Guided Anti-Predator Behavior, *Int. J Bifurcat. Chaos*, **27** (2017), 1750099. https://doi.org/10.1142/S0218127417500997

9. S. G. Mortoja, P. Panja, S. K. Mondal, Dynamics of a predator-prey model with stage-structure on both species and anti-predator behavior, *Inform. Med. Unlocked*, **10** (2018), 50–57. https://doi.org/10.1016/j.imu.2017.12.004

10. K.D. Prasad, B. Prasad, Qualitative analysis of additional food provided predator-prey system with anti-predator behaviour in prey, *Nonlinear Dyn.*, **96** (2019), 1765–1793. https://doi.org/10.1007/s11071-019-04883-0

11. S. Sirisubtawee, N. Khansai, A. Charoenloedmongkhon, Investigation on dynamics of an impulsive predator-prey system with generalized Holling type IV functional response and anti-predator behavior, *Adv. Differ. Equ.*, **2021** (2021), 160. https://doi.org/10.1186/s13662-021-03324-w

12. Y. Tian, Y. Gao, Qualitative Analysis and Feedback Control of Predator-Prey Model with Anti-predation Effect, *J. Xinyang Normal Univer. (Nat. Sci. Edit.)*, **35** (2022), 523–527. https://doi.org/10.3969/j.issn.1003-0972.2022.04.002

13. Y. F. Lv, R. Yuan, Y. Z. Pei, A prey-predator model with harvesting for fishery resource with reserve area, *Appl. Math. Model.*, **37** (2013), 3048–3062. https://doi.org/10.1016/j.apm.2012.07.030

14. D. P. Hu, H. J. Cao, Stability and bifurcation analysis in a predator-prey system with Michaelis-Menten type predator harvesting, *Nonlinear Anal.-Real.*, **33** (2017), 58–82. https://doi.org/10.1016/j.nonrwa.2016.05.010

15. T. K. Ang, H. M. Safuan, Dynamical behaviors and optimal harvesting of an intraguild prey-predator fishery model with Michaelis-Menten type predator harvesting, *Biosystems*, **202** (2021), 104357. https://doi.org/10.1016/j.biosystems.2021.104357

16. M. Costa, E. Kaszkurewicz, A. Bhaya, L. Hsu, Achieving global convergence to an equilibrium population in predator–prey systems by the use of a discontinuous harvesting policy, *Ecol. Model.*, **128** (2000), 89–99. https://doi.org/10.1016/S0304-3800(99)00220-3

17. X.Y Song, Y.F. Li, Dynamic complexities of a Holling II two-prey one-predator system with impulsive effect, *Chaos Soliton Fract*, **33** (2007), 463–478. https://doi.org/10.1016/j.chaos.2006.01.019

18. Y. Zhang, S.J. Gao, S.H. Chen, Modelling and analysis of a stochastic nonautonomous predator-prey model with impulsive effects and nonlinear functional response, *Math. Biosci. Eng.*, **18** (2021), 1485–1512. https://doi.org/10.3934/mbe.2021077

19. L. F. Nie, Z. D. Teng, H. Lin, J. G. Peng, The dynamics of a Lotka-Volterra predator-prey model with state dependent impulsive harvest for predator, *Biosystems*, **98** (2009), 67–72. https://doi.org/10.1016/j.biosystems.2009.06.001

20. H.J. Guo, L.S. Chen, X.Y. Song, Qualitative analysis of impulsive state feedback control to an algae-fish system with bistable property, *Appl. Math. Comput.*, **271** (2015), 905–922. https://doi.org/10.1016/j.amc.2015.09.046

21. Y. Tian, Y. Gao, K. B. Sun, Global dynamics analysis of instantaneous harvest fishery model guided by weighted escapement strategy, *Chaos Soliton. Fract.*, **164** (2022), 112597. https://doi.org/10.1016/j.chaos.2022.112597

22. P. S. Simenov, D. D. Bainov, Orbital stability of the periodic solutions of autonomous systems with impulse effect, *Int. J. Syst. Sci.*, **19** (1988), 2561–2585. https://doi.org/10.1080/00207728808547133

23. Y. Tian, K. B. Sun, L. S. Chen, Geometric approach to the stability analysis of the periodic solution in a semi-continuous dynamic system, *Int. J. Biomath.*, **7** (2014), 1450018. https://doi.org/10.1142/S1793524514500181

24. L.S. Chen, X. Y. Liang, Y. Z. Pei, The periodic solutions of the impulsive state feedback dynalical system, *Commun. Math. Biol. Neurosci.*, **2018** (2018), 14. https://doi.org/10.28919/cmbn/3754

25. S. Y. Tang, W. H. Pang, R. A. Cheke, J. H. Wu, Global dynamics of a state-dependent feedback control system, *Adv. Differ. Equ.*, **2015** (2015), 322. https://doi.org/10.1186/s13662-015-0661-x

26. S.Y. Tang, L.S., Modelling and analysis of integrated pest management strategy, *Discrete Cont. Dyn. B*, **4** (2004), 759–768. https://doi.org/10.3934/dcdsb.2004.4.759

27. S.Y. Tang, Y.N. SY, L.S. Chen, R.A. Cheke, Integrated pest management models and their dynamical behaviour, *B. Math. Biol.*, **67** (2005), 115–135. https://doi.org/10.1016/j.bulm.2004.06.005

28. S.Y. Tang, R.A. Cheke, State-dependent impulsive models of integrated pest management (IPM) strategies and their dynamic consequences, *J. Math. Biol.*, **50** (2005), 257–292. https://doi.org/10.1007/S00285-004-0290-6

29. K.B. Sun, T.H. Zhang, Y. Tian, Theoretical study and control optimization of an integrated pest management predator-prey model with power growth rate, *Math. Biosci.*, **279** (2016), 13–26. https://doi.org/10.1016/j.mbs.2016.06.006

30. K.B. Sun, T.H. Zhang, Y. Tian, Dynamics analysis and control optimization of a pest management predator-prey model with an integrated control strategy, *Appl. Math. Comput.*, **292** (2017), 253-271. https://doi.org/10.1016/j.amc.2016.07.046

31. Q.Q. Zhang, B. Tang, S.Y. Tang, Vaccination threshold size and backward bifurcation of SIR model with state-dependent pulse control, *J. Theor. Biol.*, **455** (2018), 75–85. https://doi.org/10.1016/j.jtbi.2018.07.010

32. Q. Zhang, B. Tang, T. Cheng, S. Tang, Bifurcation analysis of a generalized impulsive Kolmogorov model with applications to pest and disease control, *SIAM J. Appl. Math.*, **80** (2020), 1796–1819. https://doi.org/10.1137/19M1279320

33. G. Pang, X. Sun, Z. Liang, S. He, X. Zeng, Impulsive state feedback control during the sulphitation reaction in process of manufacture of sugar, *Int. J. Biomath.*, **13** (2020), 2050076. https://doi.org/10.1142/S179352452050076X

34. S. Y. Tang, B. Tang, A. L. Wang, Y. N. Xiao, Holling II predator-prey impulsive semi-dynamic model with complex Poincaré map, *Nonlinear Dyn.* **81** (2015), 1575-1596. https://doi.org/10.1007/s11071-015-2092-3

35. T. Q. Zhang, W. B. Ma, X. Z. Meng, T. H. Zhang, Periodic solution of a prey-predator model with nonlinear state feedback control, *Appl. Math. Comput.*, **266** (2015), 95-107. https://doi.org/10.1016/j.amc.2015.05.016

36. Q. Z. Xiao, B. X. Dai, Heteroclinic bifurcation for a general predator-prey model with Allee effect and state feedback impulsive control strategy, *Math. Biosci. Eng.*, **12** (2015), 1065–1081. https://doi.org/10.3934/mbe.2015.12.1065

37. J. Yang, Y. S. Tan, Effects of pesticide dose on Holling II predator-prey model with feedback control, *J. Biol. Dynam.*, **12** (2018), 527–550. https://doi.org/10.1080/17513758.2018.1479457

38. Z.Z. Shi, H. D. Cheng, Y. Liu, Y. H. Wang, Optimization of an integrated feedback control for a pest management predator-prey model, *Math. Biosci. Eng.* **16** (2019), 7963–7981. https://doi.org/10.3934/mbe.2019401

39. J. Xu, M.Z. Huang, X.Y. Song, Dynamical analysis of a two-species competitive system with state feedback impulsive control, *Int. J. Biomath.*, **13** (2020), 2050007. https://doi.org/10.1142/S1793524520500072

40. S. Tang, C. Li C; B. Tang, X. Wang, Global dynamics of a nonlinear state-dependent feedback control ecological model with a multiple-hump discrete map, *Commun. Nonlinear Sci. Numer. Simul.*, **79** (2019), 104900. https://doi.org/10.1016/j.cnsns.2019.104900

41. M. Zhang, Y. Zhao, X.Y. Song, Dynamics of bilateral control system with state feedback for price adjustment strategy, *Int. J. Biomath.* **14** (2021), 2150031. https://doi.org/10.1142/S1793524521500315

42. J. Yang, S.Y. Tang, Holling type II predator–prey model with nonlinear pulse

as state-dependent feedback control, *J. Comput. Appl. Math.*, **291** (2016), 225–241. https://doi.org/10.1016/j.cam.2015.01.017

43. Y. Tian, S. Y. Tang, R. A. Cheke, Nonlinear state-dependent feedback control of a pest-natural enemy system, *Nonlinear Dyn.* **94** (2018), 2243–2263. https://doi.org/10.1007/s11071-018-4487-4
44. Y. Tian, S. Y. Tang, Dynamics of a density-dependent predator-prey biological system with nonlinear impulsive control, *Math. Biosci. Eng.*, **18** (2021), 7318–7343. https://doi.org/10.3934/mbe.2021362
45. Y. Tian, H. M. Li, The Study of a Predator-Prey Model with Fear Effect Based on State-Dependent Harvesting Strategy, *Complexity*, **2022** (2022), 9496599. https://doi.org/10.1155/2022/9496599
46. W. Li, J. Ji, L. Huang, Global dynamic behavior of a predator-prey model under ratio-dependent state impulsive control, *Appl. Math. Model.*, **77** (2020), 1842–1859. https://doi.org/10.1016/j.apm.2019.09.033
47. W. Li, L. Huang, Z. Guo, J. Ji, Global dynamic behavior of a plant disease model with ratio dependent impulsive control strategy, *Math. Comput. Simulat.*, **177** (2020), 120–139. https://doi.org/10.1016/j.matcom.2020.03.009
48. Q.Q. Zhang,S.Y. Tang, Bifurcation analysis of an ecological model with nonlinear state-dependent feedback control by Poincaré map defined in phase set, *Commun. Nonlinear Sci. Numer. Simul.*, **108** (2022), 106212. https://doi.org/10.1016/j.cnsns.2021.106212
49. Y.Z. Wu, G.Y. Tang, C.C. Xiang, Dynamic analysis of a predator-prey state-dependent impulsive model with fear effect in which action threshold depending on the prey density and its changing rate, *Math. Biosci. Eng.*, **19** (2022), 13152–13171. https://doi.org/10.3934/mbe.2022615
50. T. Y. Li, J. A. Yorke, Period three implies chaos, *Amer. Math.*, **82** (1975), 985–992. Available from: `https://link.springer.com/chapter/10.1007/978-0-387-21830-4_6`

AIMS Press